Journal of Renewable Materials

Tech Science Press

Numerical Modelling of the Transient Hygroscopic Behavior of Flax-Epoxy Composite

Wajdi Zouari[1,*], Mustapha Assarar[1], Abderrazak Chilali[2], Rezak Ayad[1] and Hocine Kebir[3]

[1]Université de Reims Champagne-Ardenne, ITheMM EA 7548, 51097, Reims, France.

[2]Ecole Nationale Préparatoire aux Etudes d'Ingéniorat, 16012, Rouïba, Algeria.

[3]Sorbonne Universités, Université de Technologie de Compiègne, Laboratoire Roberval (UMR 7337), 60205, Compiègne, France.

[*]Corresponding Author: Wajdi Zouari. Email: wajdi.zouari@univ-reims.fr.

Abstract: This contribution deals with the development of a three-node triangular plane finite element to analyze the transient hygroscopic behavior of 2/2 twill flax fabric-reinforced epoxy composite. Several plates of this material were fabricated using the vacuum infusion process and composite specimens were then cut and aged in tap water at room temperature until saturation. To simplify, a plane modelling of water diffusion in the aged specimens is adopted and Fick's model is used to describe the water diffusion kinetics. To highlight the heterogeneity of the flax-epoxy samples, the twill flax fabrics waviness is modelled with a sinusoidal undulation. In particular, we show that the proposed finite element formulation allows estimating the flax fiber radial diffusion coefficient by an inverse approach.

Keywords: Flax-epoxy composite; water ageing; fick's model; finite element analysis

1 Introduction

Over the past two decades, the environmental requirements have encouraged several research and development works to find an ecological alternative to traditional oil-based composite materials, in particular those reinforced with glass fibers. Within this context, natural fiber-reinforced polymer composites and especially those reinforced with flax fibers have gained ground in several industrial areas such as automotive, aeronautic, sports, packaging and construction industries [1-3]. In fact, natural fibers combine multiple advantages such as their interesting specific mechanical properties and especially their availability and biodegradability which constitute a major guarantee with respect to environment constraints [4,5]. However, their hydrophilic nature remains the major drawback to their development in semi-structural and structural applications exposed to a wet environment. Indeed, several research works have already shown that the exposure of natural fiber-reinforced composites to humidity induces an important variation of their mechanical and dynamical properties (see [6-15] among others). These variations are principally related to the swelling of natural fibers due to moisture absorption, which causes different degradations particularly at the fiber-matrix interface and consequently reduces the sustainability of these composite materials. Therefore, the control of these variations passes by the understanding of diffusion kinetics within natural fiber-reinforced polymer composites. Within this context, many research works have focused on these aspects by analyzing the behavior of natural fiber-reinforced composites in wet environment using one-dimensional (1D) Fick's model [8,16-18]. However, this approximation cannot be sufficient in some cases due to the anisotropic nature of the natural fiber, which makes the water diffusion process more complex. Therefore, it remains necessary to take into account the three-dimensional (3D) effects in order to better understand water diffusion kinetics in natural fiber reinforced composite materials. To this end, 3D Fick's model has been considered in some works [19,20] to identify

the 3D moisture diffusion coefficients. For example, Chilali et al. [20] showed that water diffusion kinetics predicted by 3D Fick's model is in good agreement with the experimental curves. Moreover, they found through the study of several geometric parameters that water diffusion in their studied flax composites is strongly influenced by the morphology of the flax fiber.

Although very practical, these analytical models permit only to study composite materials at their macroscopic scale and for simple geometrical shapes. It is for example difficult to find an analytical solution of 3D Fick's law for an anisotropic material as discussed in [20]. In addition, the analytical models do not allow to predict the diffusion behavior of the composite constituents like the diffusion properties of natural fibers which are relatively difficult to measure experimentally. In this case, the use of a numerical model could outweigh these limitations as it allows for instance to estimate the moisture content at any point of a composite structure with complex shape.

In the literature, several works have dealt with the finite element modelling of moisture diffusion particularly in synthetic fiber-reinforced polymer composites [21-27]. In these latter papers, finite element simulations have been conducted at the microscopic level of the composite materials to take into account their heterogeneity. For example, Joliff et al. [23] used a 2D finite element model to simulate water diffusion in unidirectional glass fiber-reinforced epoxy composites aged at 70°C in deionized water up to 16 weeks. In particular, they modelled the fiber-matrix interphase and studied the influence of glass fibers distribution with and without barrier effects on the diffusion kinetics of the glass-epoxy composite. Joliff et al. [23] showed that the matrix diffusion coefficient must be higher than that of the bulk epoxy resin to correctly fit the experimental water uptake curve which indicates that the epoxy diffusivity behavior is highly modified by the presence of glass fibers. Contrary to synthetic fiber-reinforced composites, the number of contributions dealing with numerical modelling of moisture diffusion in natural fiber-reinforced composites remains limited. Among these contributions, we cite the work by Regazzi et al. [27] which concerns numerical modelling of moisture diffusion in short flax-PLA composites aged in water at different temperatures. In this latter contribution, the studied composite material was assumed homogeneous to simplify the finite element analysis.

In this work, we present the formulation of a three-node triangular membrane finite element to analyze the transient hygroscopic behavior of 2/2 twill flax fabric-reinforced epoxy composite aged in tap water at room temperature. For this purpose, Fick's model is considered to describe the diffusion kinetics within the flax-epoxy composite specimens and their heterogeneity is also taken into consideration by modelling the twill flax fabrics waviness with a sinusoidal undulation.

The present paper is structured as follows. After the introduction, we present in Section 2 the experimental water uptake curve of the flax-epoxy composite. Section 3 is devoted to the finite element approximation of the hygroscopic problem and presents the formulation of the hygroscopic three-node membrane element. Before the concluding remarks, we discuss in Section 4 the obtained numerical results.

2 Experimental Water Absorption Curve

In this work, the hygroscopic behavior of 2/2 twill flax fabric-reinforced epoxy composite is investigated. The flax fabrics were provided by Depestele group and present an aerial weight of 330 g/m^2 and a fiber density of 1450 kg/m^3. The epoxy resin is the SR 8100 and was provided with its SD 88225 hardener by Sicomin. Several flax-epoxy laminate plates of dimensions 200 × 200 × 3 mm^3 were prepared by the vacuum infusion process (see [20,28] for more details about the fabrication process). To obtain a thickness of 3 mm, four layers of flax fabrics were used. After that, the flax-epoxy plates were cut and shaped in square specimens of side 20 mm. Then, the obtained specimens were totally immersed into tap water at room temperature to accelerate their water absorption kinetics. During their ageing, the weight variation of each composite specimen was measured and the moisture absorption rate was determined by the following expression:

$$M_t = \frac{W_t - W_0}{W_0} \times 100\% \quad (1)$$

where W_0 is the dry initial weight of each specimen and W_t is its weight at time t.

The experimental water uptake curve of the flax-epoxy specimens is shown in Fig. 1. Initially, the water absorbed by these samples increases quasi-linearly with the ageing time and then slows down before reaching the equilibrium after 60 days of ageing. This diffusivity behavior can be described by Fick's model [29].

The macroscopic diffusion coefficients D_1, D_2 and D_3 of the flax-epoxy specimens are summarized in Tab. 1 where 1 is the warp direction, 2 is the weft direction and 3 is the thickness direction. These parameters were identified by minimizing the quadratic error between the analytical solution of 3D Fick's model and the experimental results of Fig. 1. In particular, we remark that water diffusion occurs principally across the thickness of the flax-epoxy samples as D_3 is found approximately 3 times the plane diffusion coefficients D_1 and D_2. This result shows that water diffuses more easily across the thickness of the composite specimens than towards their plane directions.

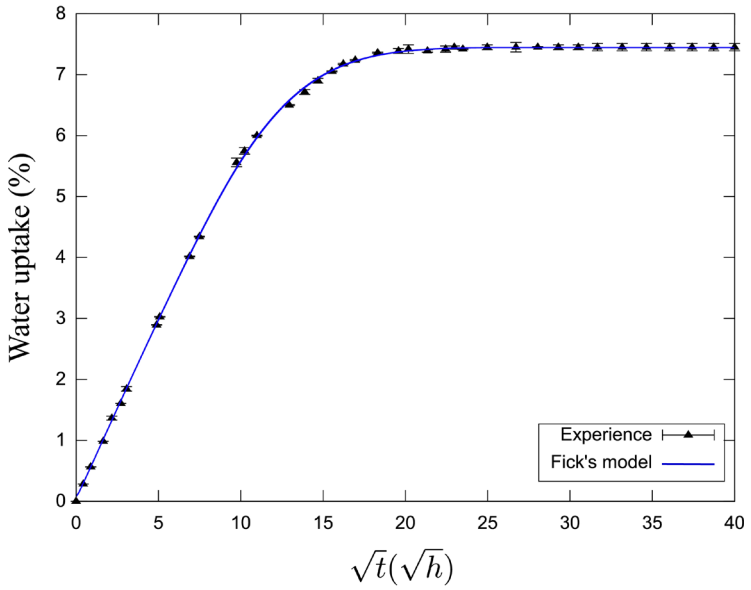

Figure 1: Experimental water uptake curve of the flax-epoxy specimens

Table 1: Diffusion coefficients of the flax-epoxy specimens determined from 3D Fick's model

D_1 ($\times 10^{-3}$ mm^2/h)	D_2 ($\times 10^{-3}$ mm^2/h)	D_3 ($\times 10^{-3}$ mm^2/h)	M_∞ (%)
3.348 ± 0.072	2.988 ± 0.108	9.936 ± 0.504	7.451 ± 0.065

3 Finite Element Approximation of the Hygroscopic Problem

We consider a 2D composite solid B_0 as shown in Fig. 2. To describe its hygroscopic behavior, we introduce the variable $c(\boldsymbol{x},t)$ which represents the moisture content at time t of one point P inside B_0 characterized by its position vector $\boldsymbol{x} \in B_0$.

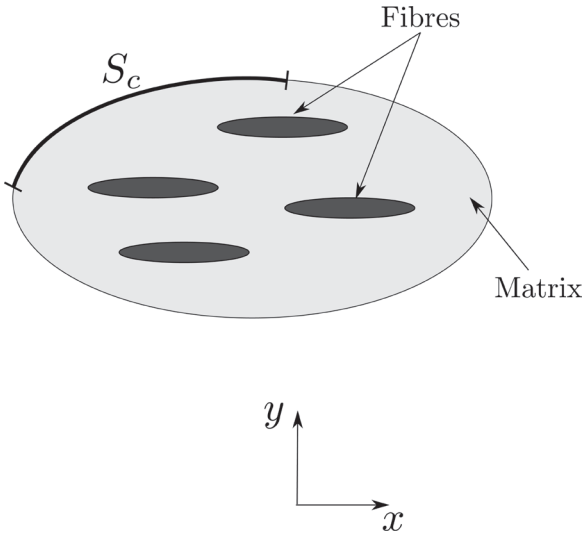

Figure 2: A 2D composite solid with moisture content boundary conditions

We recall that Fick's model is considered to describe water diffusion kinetics in the flax-epoxy specimens:

$$\frac{\partial c}{\partial t} = \mathrm{div}(\boldsymbol{D}.\nabla c) \qquad \text{with} \qquad c = c_{imp} \quad \text{on} \quad S_c \tag{2}$$

where c is the moisture concentration and $\boldsymbol{D}$ is the diffusion tensor which is supposed symmetric.

For plane problems, $\boldsymbol{D}$ and the gradient of the moisture concentration ∇c are given by:

$$\boldsymbol{D} = \begin{bmatrix} D_x & D_{xy} \\ D_{xy} & D_y \end{bmatrix} \qquad \text{and} \qquad \nabla c = \begin{Bmatrix} \dfrac{\partial c}{\partial x} \\ \dfrac{\partial c}{\partial y} \end{Bmatrix} \tag{3}$$

where D_x and D_y are the diffusion coefficients along the x and y directions, respectively, while D_{xy} represents the diffusion rate in the x-direction due to a moisture concentration gradient in the y-direction.

The weak form of the diffusion Eq. (2) is obtained by introducing a test function c^* that verifies $c^* = 0$ on S_c:

$$w(c, c^*) = \int_{B_0} \left(\dot{c} - \mathrm{div}(\boldsymbol{D}.\nabla c) \right) c^* \, dV = 0 \quad \forall c^* \quad \text{with} \quad \dot{c} = \frac{\partial c}{\partial t} \tag{4}$$

By remarking that

$$c^* \mathrm{div}(\boldsymbol{D}.\nabla c) = \mathrm{div}(c^* \boldsymbol{D}.\nabla c) - \nabla c^* . \boldsymbol{D}.\nabla c, \tag{5}$$

the weak form of Fick's diffusion equation becomes

$$w(c, c^*) = \int_{B_0} \dot{c} c^* \, dV + \int_{B_0} \nabla c^* . \boldsymbol{D}.\nabla c \, dV + \int_{\partial B_0} c^* \phi_n \, dS = 0 \qquad \forall c^* \tag{6}$$

where ϕ_n is the normal diffusion flux and ∂B_0 is the boundary of the 2D composite domain B_0.

The finite element approximation of the weak form (6) necessitates spatial and time discretizations. To this end, the heterogeneous plane composite domain B_0 is firstly divided into three-node plane elements for spatial discretization and secondly, the backward Euler integration scheme is adopted for time integration.

The proposed hygroscopic plane element is shown in Fig. 3. The following interpolation functions $N_1 = 1-\xi-\eta$, $N_2 = \xi$ and $N_3 = \eta$ associated with the classical three-node membrane element are used to approximate the moisture content within the hygroscopic plane element in terms of the nodal variables:

$$c = \sum_{i=1}^{3} N_i(\xi,\eta)c_i \tag{7}$$

where c_i are the nodal moisture contents.

Using the finite element approximation (7), it is possible to show that c and ∇c are related to the nodal degrees of freedom vector $\boldsymbol{c}_n$ as

$$c = {}^t\boldsymbol{N}_c \cdot \boldsymbol{c}_n \quad ; \quad \nabla c = \boldsymbol{B}_c \cdot \boldsymbol{c}_n \tag{8}$$

At the element level, the finite element approximation of the weak form (6) reads

$$w^e(\boldsymbol{c}_n, \boldsymbol{c}_n^*) = {}^t\boldsymbol{c}_n^* \cdot \Big[\int_{B_0} \boldsymbol{N}_c^{?} \boldsymbol{N}_c \, dV \cdot \dot{\boldsymbol{c}}_n + \int_{B_0} \boldsymbol{B}_c \cdot \boldsymbol{C} \cdot {}^t\boldsymbol{B}_c \, dV \cdot \boldsymbol{c}_n + \int_{\partial B_0} \boldsymbol{N}_c \phi_n \, dS \Big] = 0 \qquad \forall \boldsymbol{c}_n^* \tag{9}$$

This approximation could be rewritten as

$$\boldsymbol{K}_c . \boldsymbol{c}_n + \boldsymbol{C} \cdot \dot{\boldsymbol{c}}_n - \boldsymbol{F}_c = 0 \tag{10}$$

with $\boldsymbol{K}_c = \int_{B_0} \boldsymbol{B}_c \cdot \boldsymbol{C} \cdot {}^t\boldsymbol{B}_c \, dV$ is the moisture diffusivity matrix, $\boldsymbol{C} = \int_{B_0} \boldsymbol{N}_c \cdot {}^t\boldsymbol{N}_c \, dV$ is the moisture velocity matrix and $\boldsymbol{F}_c = -\int_{\partial B_0} \boldsymbol{N}_c \phi_n \, dS$.

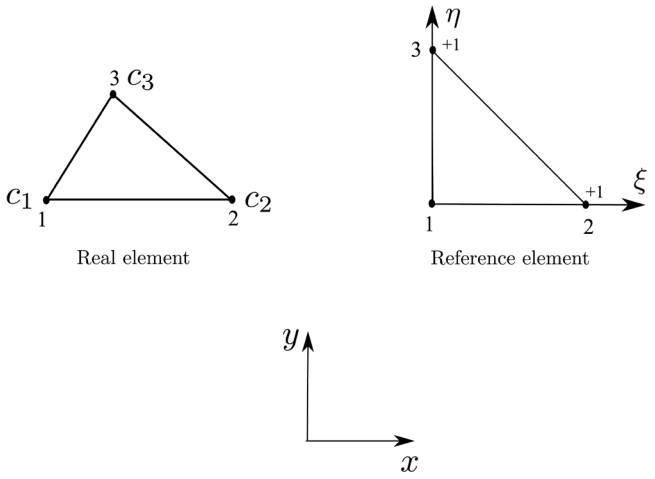

Figure 3: The three-node hygroscopic membrane element

For time integration of Eq. (10), the loading interval $[t, t+\Delta t]$ is considered. The backward Euler integration of Eq. (10) gives the residual vector at $t+\Delta t$:

$$\boldsymbol{R} = \boldsymbol{K}_c \cdot \boldsymbol{c}_n^{\,t+\Delta t} + \boldsymbol{C} \cdot \frac{\Delta \boldsymbol{c}_n}{\Delta t} - \boldsymbol{F}_c^{\,t+\Delta t} \quad \text{with} \quad \Delta \boldsymbol{c}_n = \boldsymbol{c}_n^{\,t+\Delta t} - \boldsymbol{c}_n^{\,t} \tag{11}$$

The elementary tangent stiffness matrix of the proposed three-node membrane element is obtained by differentiating the residual vector $\boldsymbol{R}$ with respect to $\Delta \boldsymbol{c}_n$ as:

$$\boldsymbol{K}_T = -\frac{\partial \boldsymbol{R}}{\partial \Delta \boldsymbol{c}_n} = -\boldsymbol{K}_c - \frac{\boldsymbol{C}}{\Delta t} \tag{12}$$

4 Numerical Results

In this section, we use the hygroscopic three-node triangular element to study the water absorption behavior of the aged flax-epoxy specimens. In particular, this study permits to obtain an approximation of the flax fiber radial diffusion coefficient and its evolution with thickness. To take account of the heterogeneity of the flax-epoxy samples, we need to describe the 2/2 twill weave of the flax fabrics as detailed in the next section.

4.1 Description of the Flax Yarn Undulation

As previously announced, the three-node hygroscopic triangle element is used in the following sections to reproduce the experimental water absorption curve of the flax-epoxy specimens. To simplify, a plane modelling of the diffusion problem is considered as depicted in Fig. 4(b).

To highlight the heterogeneity of the flax-epoxy samples, a sinusoidal model is considered to describe the 2/2 twill weave of the flax fabrics. The 3 mm thick flax-epoxy specimens are constituted of four layers of flax fabrics. Owing to symmetry, only one-fourth of the cross section of each composite specimen is modelled as shown in Fig. 4(b) This corresponds to a unit cell of the 2/2 twill flax fabric. Moreover, the twill flax fabrics used in this study are balanced and accordingly the warp and weft directions (directions x and y in Fig. 4(a) are considered identical.

The geometrical model used to describe the flax yarn undulation is based on sinusoidal functions. In the warp direction (direction x), the flax strand undulation within the modelled $10 \times 1.5\,\text{mm}^2$ plane section can be approximated by the following function [30]:

$$H(x) = \begin{cases} \frac{h}{2}\sin\left(\frac{\pi}{a}(x+a)\right) & x \in [0, \frac{a}{2}] \cup [\frac{7a}{2}, 4a] \\ -\frac{h}{2} & x \in [\frac{a}{2}, \frac{3a}{2}] \\ -\frac{h}{2}\sin\left(\frac{\pi}{a}(x+a)\right) & x \in [\frac{3a}{2}, \frac{5a}{2}] \\ \frac{h}{2} & x \in [\frac{5a}{2}, \frac{7a}{2}] \end{cases} \tag{13}$$

where a and h are defined in Fig. 4(c) and correspond to the width and thickness of the flax fiber strand, respectively ($a = 2.5\,\text{mm}$ in our case).

The geometry of the flax fiber strand is then approximated by the following sinusoidal function:

$$z(x) = \frac{h}{2}\sin(\frac{\pi}{a}x) \tag{14}$$

This function is used to calculate the cross section of the flax fiber strand as:

$$S = 2\int_0^a \frac{h}{2}\sin(\frac{\pi}{a}x)dx = \frac{2ah}{\pi} \tag{15}$$

The cross Section S and the perimeter of the warp flax strand allow then to calculate the total surface of the flax fiber reinforcement that respects the fiber volume fraction of the flax-epoxy specimens (32%).

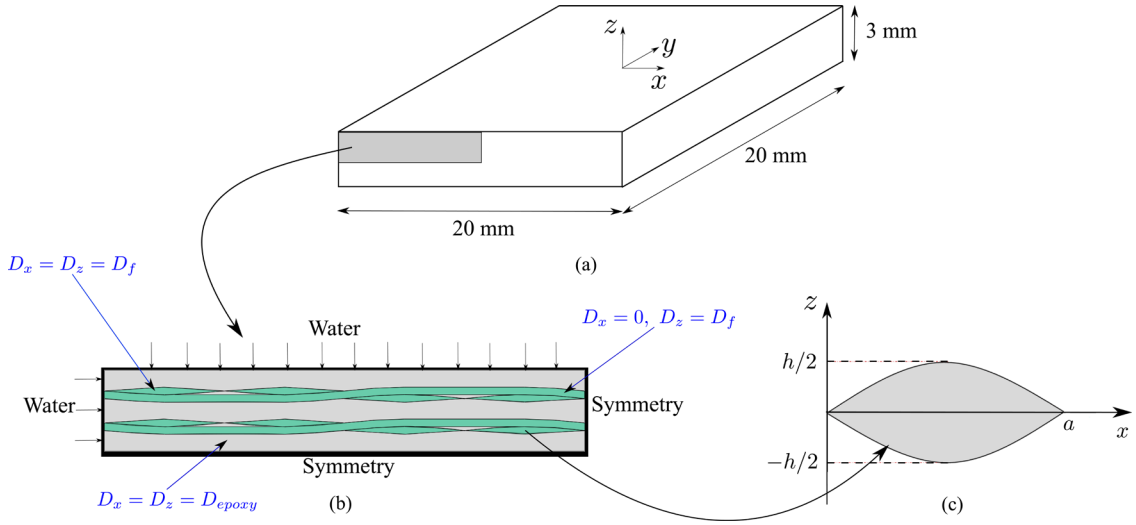

Figure 4: (a) A $20 \times 20 \times 3\,\text{mm}^3$ flax-epoxy specimen. (b) Plane modelling of water diffusion within the flax-epoxy specimen. (c) Sinusoidal modelling of the flax fiber strand

4.2 Hygroscopic Behavior of the Flax-Epoxy Composite

To model water diffusion within the heterogeneous flax-epoxy composite specimens (Fig. 4(b)), we need the diffusion coefficients of the epoxy resin and the flax fiber. The diffusion coefficient of the epoxy resin can be deduced from its experimental water absorption curve. It presents a Fickian behavior and the minimization of the quadratic error between the analytical solution of Fick's model and the experimental results gives an isotropic diffusion behavior characterized by $D_{\text{epoxy}} = 5.220 \times 10^{-3}\,\text{mm}^2/\text{h}$. For the flax fiber, we recall that it is difficult to measure its radial and longitudinal diffusion coefficients experimentally. As water diffusion occurs principally across the thickness of the flax-epoxy specimens as shown in Tab. 1, we neglect in this study the longitudinal diffusion coefficient of the flax fiber in order to facilitate the estimation of its radial coefficient designated by D_f in the following. Consequently, we use $D_x = 0$ and $D_z = D_f$ for the warp direction and $D_x = D_z = D_f$ for the weft direction as depicted in Fig. 4(b).

To obtain a first approximation of the flax fiber radial diffusion coefficient, we use the homogenization model of Halpin-Tsai [31] largely considered in the case of synthetic fiber-reinforced composites:

$$D_t = D_{\text{epoxy}} \frac{1+\zeta\eta V_f}{1-\eta V_f} \quad \text{with} \quad \eta = \frac{D_f - D_{\text{epoxy}}}{D_f + D_{\text{epoxy}}} \quad \text{and} \quad \zeta = 1 \tag{16}$$

where D_t is the transverse (across the thickness) diffusion parameter of the flax-epoxy specimens, D_f is the flax fiber radial diffusion coefficient and V_f is the flax fiber volume fraction. It is also important to note that ζ is a measure of the reinforcement geometry and is taken equal to 1 in this work to simplify.

The resolution of Eq. (16) allows obtaining a first estimation of the flax fiber radial diffusion coefficient $D_f = 0.372$ mm^2 /h. The diffusion coefficients D_f and D_{epoxy} are now used with the refined finite element model of Fig. 5 to simulate water diffusion within the flax-epoxy specimens. This refined mesh of 45,000 three-node elements was obtained after a mesh convergence study. The moisture boundary conditions are applied to the top and left edges of the 2D model ($c = M_\infty = 7.451\%$).

Fig. 6 shows a comparison between the experimental and numerical absorption curves of the flax-epoxy specimens. It is important to note that the numerical water absorption curve of Fig. 6 is the arithmetic average of all nodal moisture concentrations of the finite element model. We remark that the numerical water absorption curve does not accurately describe the experimental results. The difference between these two curves reflects the difficulty to predict the flax-epoxy diffusion behavior using a heterogeneous model.

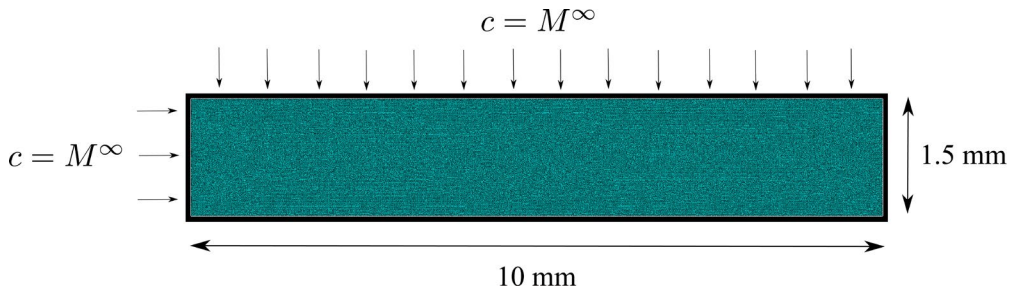

Figure 5: Finite element modelling of water diffusion within the flax-epoxy specimens using 45,000 three-node triangular plane elements

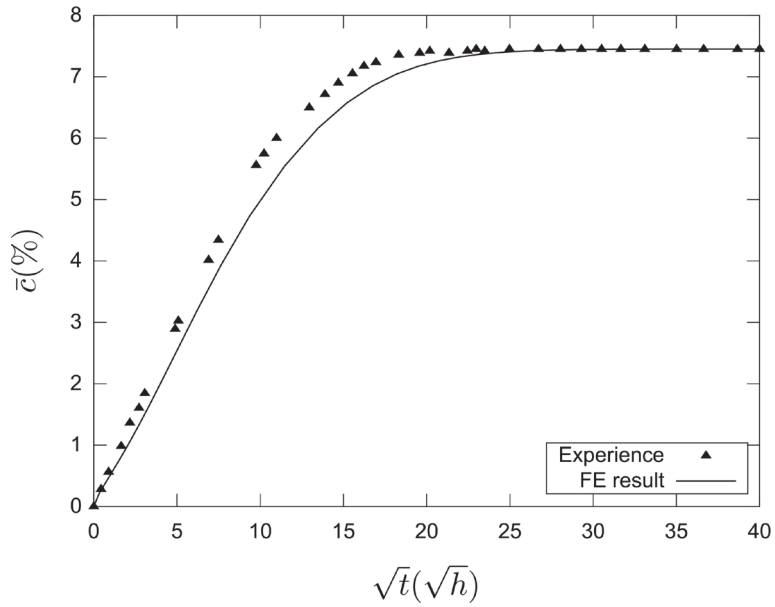

Figure 6: Comparison between the experimental and numerical water absorption curves of the flax-epoxy specimens using $D_{\text{epoxy}} = 5.220 \times 10^{-3}$ mm^2/h and $D_f = 0.372$ mm^2/h

To better fit the experimental water absorption curve of the flax-epoxy specimens, three combinations of the epoxy resin and the flax fiber diffusion coefficients are proposed. In the first combination, we fix the epoxy resin diffusion coefficient ($D_{\text{epoxy}} = 5.220 \times 10^{-3}$ mm^2/h) and vary the flax fiber radial coefficient so as to fit the experimental curve. In the second combination, we vary the

epoxy resin diffusivity coefficient and we use the initial estimation of the flax fiber radial diffusion coefficient ($D_f = 0.372$ mm^2/h). In the third combination, we consider the average values of the first and second combinations. Fig. 7 shows the results of the three combinations.

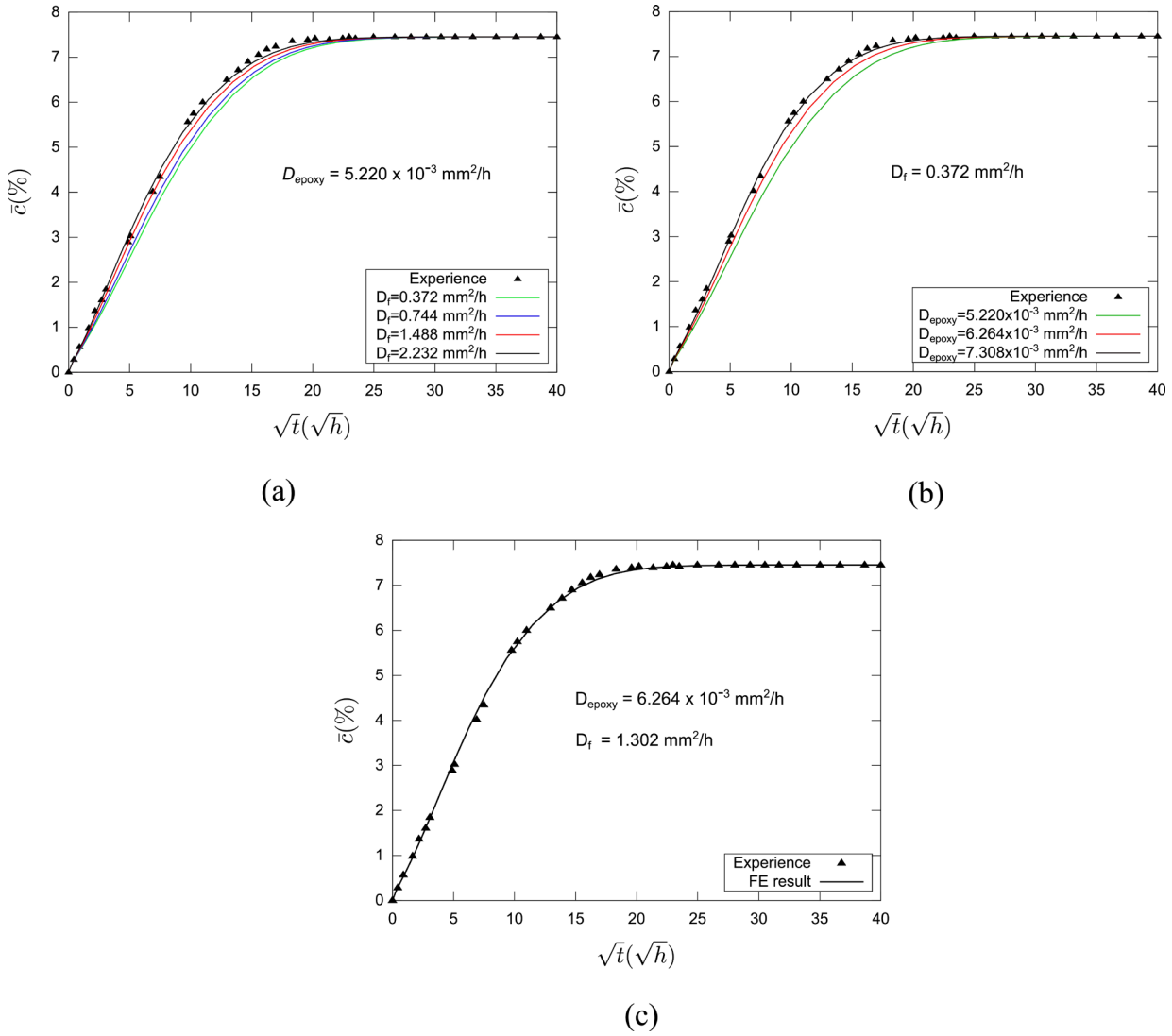

Figure 7: Numerical water absorption curves of the flax-epoxy specimens obtained by: (a) varying the flax fiber radial diffusion coefficient, (b) varying the epoxy matrix diffusion coefficient and (c) using the average values of the first and second combinations

The first and second combinations permit to perfectly fit the experimental water uptake curve of the flax-epoxy specimens. The third combination using the average coefficients $\bar{D}_f = 1.302$ mm^2/h and $\bar{D}_{epoxy} = 6.264 \times 10^{-3}$ mm^2/h also allows to accurately describe the experimental curve. These results clearly show that the water diffusion coefficient of the epoxy resin (and even that of the flax fiber) should be adjusted from that of the pure epoxy resin to correctly predict the diffusivity behavior of the flax-epoxy specimens. This tendency has been already reported in the literature in the case of synthetic fiber-reinforced composites [24,32]. In Joliff et al. [24] for example, the diffusion coefficient of the epoxy

matrix was found at minimum 30% larger than that of the bulk epoxy resin in order to fit the experimental water uptake curve of unidirectional glass fiber-reinforced epoxy specimens.

This difference in the value of D_{epoxy} (+ 22% in our case) could be explained by the fact that much more defects appear in the flax-epoxy specimens when compared with the pure epoxy resin samples and they are related firstly to the presence of porosities in the flax-epoxy specimens (the porosity content is approximately equal to 5%) and secondly to the microcracks principally located at the fiber-matrix interface (Fig. 8(a)). In addition to that, the flax fiber is known to be much more hydrophilic than the epoxy resin which induces a differential swelling between the reinforcement and the matrix and leads to more microcracks at the fiber-matrix interface (Fig. 8(a)). Moreover, the flax fiber morphology and microstructure offer many interfaces which increase water diffusion in the flax-epoxy specimens (Figs. 8(b) and 8(c)). All these defects make the epoxy matrix less resistant to water diffusion than the pure epoxy resin and explains in part the difference in D_{epoxy}. For the flax fiber, the results of Fig. 7 permit to obtain a more accurate approximation of its radial diffusion coefficient than that deduced from the Halpin-Tsai model (Eq. (16)).

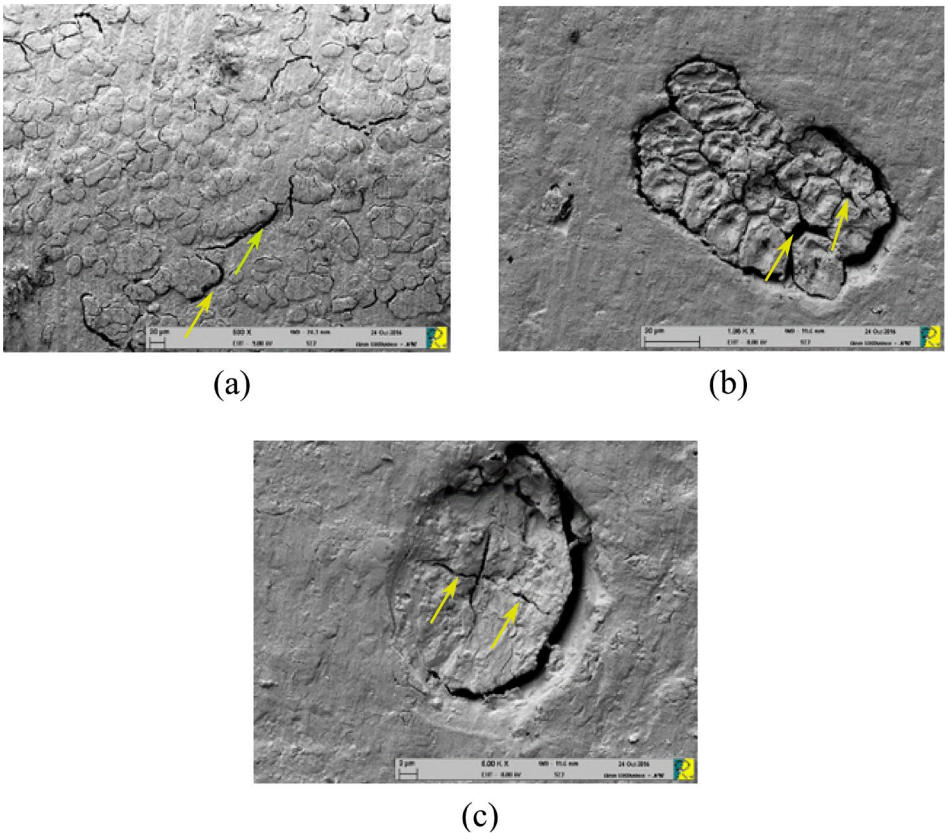

Figure 8: Microscopic observations on aged flax-epoxy specimens: (a) microcracks at the fiber-matrix interfaces, (b) microcracks between flax fibers of the same bundle and (c) microcracks inside the flax fiber

4.3 Effect of Thickness

In this last section, we study the effect of thickness on the diffusion behavior of the flax-epoxy specimens. The thickness effect has been already experimentally investigated by Chilali et al. [20] in addition to other geometric parameters. To this end, several flax-epoxy plates of dimensions $200 \times 200 \times 3$, $200 \times 200 \times 4$, $200 \times 200 \times 6$, $200 \times 200 \times 8$ and $200 \times 200 \times 10$ mm^3 were prepared by the vacuum infusion process. They were then cut and shaped in square specimens of side 20 mm. All samples edges were sealed except top and bottom faces in order to force water diffusion across

the thickness [20]. Fig. 9 shows the experimental water uptake curves of the sealed flax-epoxy specimens and Tab. 2 summarizes their diffusion coefficients across the thickness and their maximum water uptakes. These transverse diffusion coefficients were identified by minimizing the quadratic error between the analytical solution of 1D Fick's model and the experimental results.

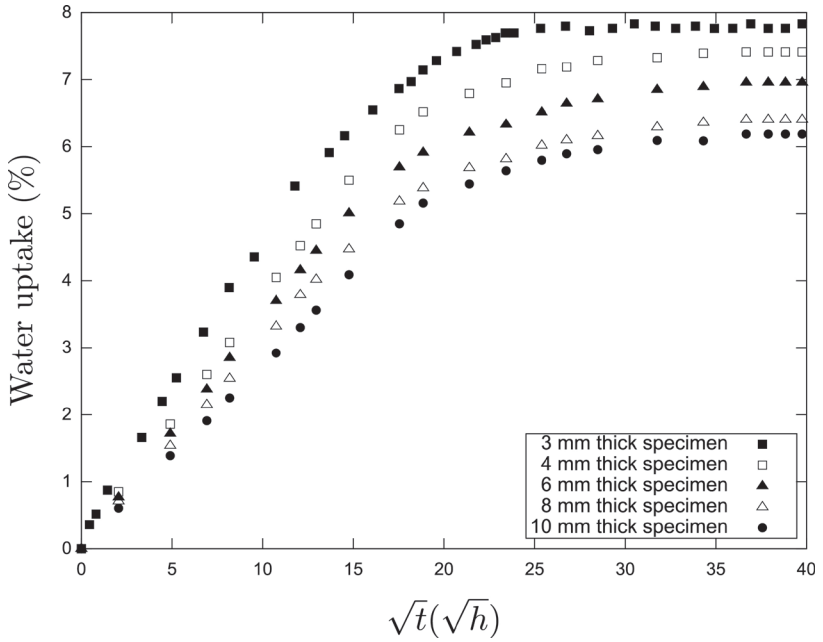

Figure 9: Experimental water uptake curves of the 3, 4, 6, 8 and 10 mm thick sealed flax-epoxy specimens with equal plane dimensions (20×20 mm^2)

Table 2: Transverse (across the thickness) diffusion coefficients and maximum water uptakes of the sealed flax-epoxy specimens

	3 mm thick	4 mm thick	6 mm thick	8 mm thick	10 mm thick
M_∞ (%)	7.832 ± 0.076	7.425 ± 0.112	6.963 ± 0.065	6.412 ± 0.092	6.187 ± 0.057
D_3 ($\times 10^{-3}$ mm^2/h)	6.264 ± 0.512	8.316 ± 0.233	17.717 ± 0.157	30.024 ± 0.344	40.576 ± 0.420

The results of Fig. 9 and Tab. 2 show a drop of water diffusion kinetics when increasing thickness characterized by a decrease of the maximum water uptake and a drop of the water absorption rate defined as the slope of the linear part of the water absorption curve. This tendency has been already reported in the literature in the case of synthetic fiber-reinforced polymer composites [33-35]. Bunsell [33] has related this phenomenon to a molecular rearrangement of the polymeric network when specimens become thicker which slows down their diffusion kinetics. Moreover, this variation of diffusion kinetics could also be related to the increasing number of epoxy resin layers enclosing the flax fabrics which may decrease water absorption across the thickness.

Contrary to the maximum water uptake and the water absorption rate, the transverse water diffusion coefficient of the flax-epoxy specimens is found to increase with thickness which shows that the flax fiber and the epoxy resin diffusion coefficients are also sensitive to thickness change. Accordingly, we propose in the following to quantify this evolution by considering the same inverse approach as Section 4.2.

Fig. 10 shows a plane modelling of water diffusion in the sealed flax-epoxy specimens. The sinusoidal model introduced in Section 4.1 is always considered to describe the 2/2 twill weave of the flax fabrics. Owing to symmetry, only one-fourth of the cross section of each flax-epoxy specimen is

modelled as shown in Fig. 10 Concerning the finite element calculations, we used for each flax-epoxy specimen a refined mesh like that of Fig. 5 after a mesh convergence study. The moisture content boundary conditions were applied only to the top edge of the 2D model as depicted in Fig. 10(a) ($c = M_\infty$). To carry out finite element simulations, we need the flax fiber and the epoxy resin diffusion coefficients. The application of the Halpin-Tsai model (Eq. (16)) allows to obtain a first approximation of these coefficients based on the transverse diffusion coefficients of Tab. 2. After that, the three combinations presented in Section 4.2 were applied to fit the experimental water absorption curves of the flax-epoxy specimens.

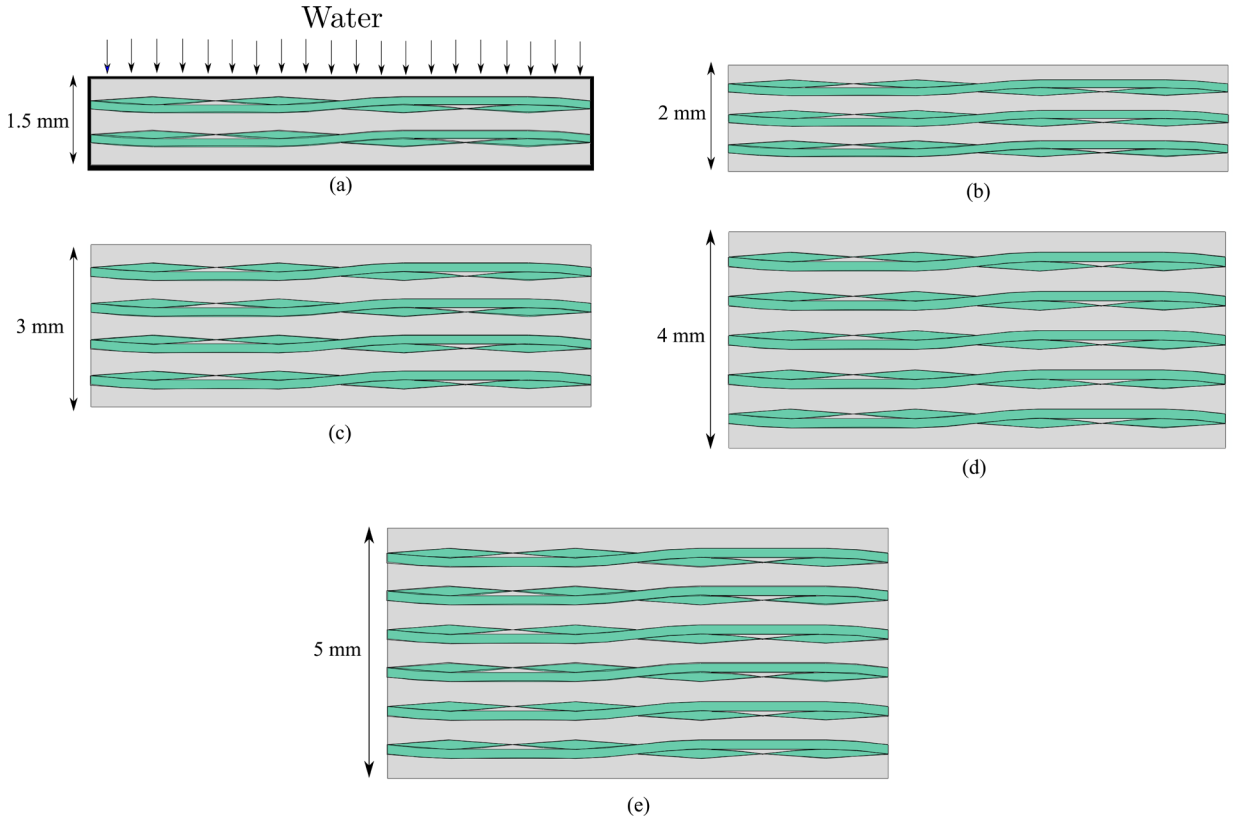

Figure 10: Plane modelling of water diffusion within the sealed flax-epoxy specimens: (a) 3 mm thick specimen (4 layers), (b) 4 mm thick specimen (6 layers), (c) 6 mm thick specimen (8 layers), (d) 8 mm thick specimen (10 layers) and (e) 10 mm thick specimen (12 layers)

We depict in Fig. 11 the evolution of the flax fiber and the epoxy resin diffusion coefficients that correctly fit the experimental water uptake curves of Fig. 9. We remark that these diffusion coefficients vary exponentially with respect to thickness with a more pronouncing evolution of the flax fiber radial coefficient. In fact, the epoxy resin diffusion coefficient of the 10 mm thick specimen is approximately 6 times greater than that of the 3 mm thick specimen while the flax fiber radial diffusion coefficient is found to increase by 13-fold from 3 mm to 10 mm thick specimens. This increase of D_f and especially that of D_{epoxy} seems to be in accordance with that of the flax-epoxy specimens (D_3 increases by 548% between the 3 mm and the 10 mm thick specimens as shown in Tab. 2). The high increase of D_f when compared with D_{epoxy} could be related to the hydrophilicity of the flax fabrics when compared with the epoxy matrix which could justify in part the more pronouncing evolution of D_f.

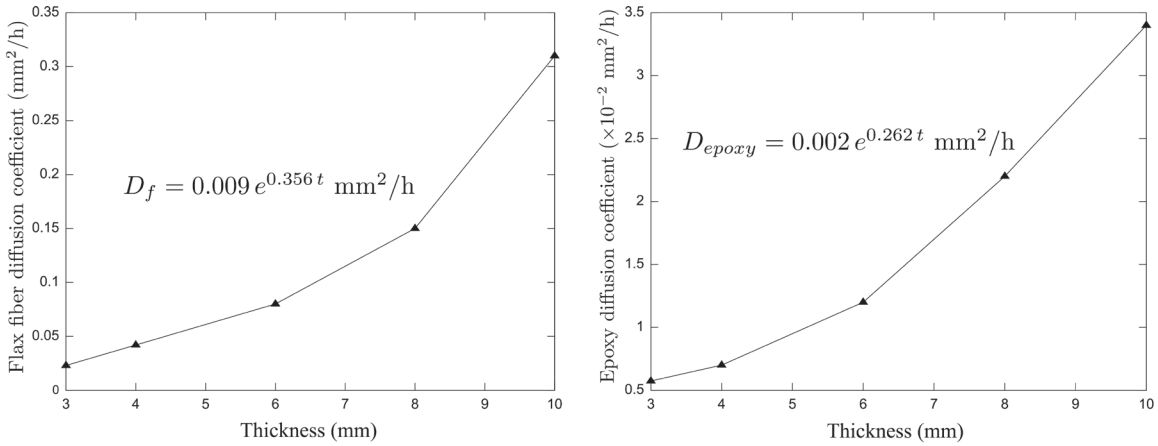

Figure 11: (a) Evolution of the flax fiber radial diffusion coefficient with respect to thickness deduced from finite element simulations (*t* designates the thickness). (b) Evolution of the epoxy resin diffusion coefficient with respect to thickness deduced from finite element simulations

4 Conclusion

In this paper, a three-node membrane finite element was developed to analyze the transient hygroscopic behavior of 2/2 twill flax fabric-reinforced epoxy composite aged in tap water at room temperature until saturation. To take into account the heterogeneity of the flax-epoxy composite in the finite element model, a sinusoidal description of the flax fabrics undulation was adopted and Fick's model was considered to describe the flax-epoxy water diffusion kinetics.

This study firstly allowed to estimate the flax fiber radial diffusion coefficient using an inverse procedure. It is worthy to recall that the flax fiber and more generally natural fibers diffusivity properties are very difficult to obtain experimentally. Secondly, we showed that the diffusion behavior of the epoxy resin is highly modified by the presence of flax fabrics. Finally, the numerical investigation of the thickness effect allowed to follow the exponential evolution of the flax fiber and the epoxy resin diffusion coefficients across the thickness.

As a future work, it would be interesting to estimate the flax fiber longitudinal diffusion coefficient using the same inverse approach. This coefficient was neglected in this study to facilitate the identification of the flax fiber radial diffusion coefficient as water diffusion was found to occur principally across the thickness of the aged flax-epoxy specimens. Besides, it would also be interesting to take account of the dependency of the flax fiber diffusion coefficients on the local moisture content.

References

1. Hess, K. M., Srubar W. V. (2015). Mechanical characterization of gelatin-flax natural-fiber composites for construction. *Journal of Renewable Materials, 3(3),* 175-182.
2. Hosseini, N., Javid, S., Amiri, A., Ulven, C., Webster, D. C. et al. (2015). Micromechanical viscoelastic analysis of flax fiber reinforced bio-based polyurethane composites. *Journal of Renewable Materials, 3(3),* 205-215.
3. Arunjunairaj, M., Günter, W., Thomas, H. S., Wolfgang, G. A. (2016). Properties of woven natural fiber-reinforced biocomposites. *Journal of Renewable Materials, 4(3),* 215-224.
4. Lawrence, M. (2001). Reducing the environmental impact of construction by using renewable materials. *Journal of Renewable Materials, 32(8),* 1105-1115.
5. Hoiby, J. C., Netravali, A. N. (2015). Can we build with plants? Cabin construction using green composites. *Journal of Renewable Materials, 3(3),* 244-258.
6. Chilali, A., Zouari, W., Assarar, M., Kebir, H., Ayad, R. (2018). Effect of water ageing on the load-unload cyclic

behaviour of flax fibre-reinforced thermoplastic and thermosetting composites. *Composite Structures, 183,* 308-319.

7. Islam, M. S., Pickering, K. L., Foreman, N. J. (2010). Influence of hygrothermal ageing on the physico-mechanical properties of alkali treated industrial hemp fibre reinforced polylactic acid composites. *Journal of Polymers and the Environment, 18(4),* 696-704.
8. Assarar, M., Scida, D., Mahi, A. E., Poilâne, C., Ayad, R. (2011). Influence of water ageing on mechanical properties and damage events of two reinforced composite materials: flax-fibres and glass-fibres. *Materials & Design, 32(2),* 788-795.
9. Le Duigou, A., Bourmaud, A., Davies, P., Baley, C. (2014). Long term immersion in natural seawater of flax/PLA biocomposite. *Ocean Engineering, 90,* 140-148.
10. Cheour, K., Assarar, M., Scida, D., Ayad, R., Gong, X. L. (2016). Effect of water ageing on the mechanical and damping properties of flax-fibre reinforced composite materials. *Composite Structures, 152, 2*59-266.
11. Kumar, A. P., Mohamed, M. N. (2018). A comparative analysis on tensile strength of dry and moisture absorbed hybrid kenaf/glass polymer composites. *Journal of Industrial Textiles, 47(8),* 2050-2073.
12. Abida, M., Gehring, F., Mars, J., Vivet, A., Dammak, F. et al. (2019). Effect of hygroscopy on non-impregnated quasi-unidirectional flax reinforcement behaviour. *Industrial Crops and Products, 28,* 315-322.
13. Habibi, M., Laperrière, L., Hassanabadi, H. M. (2019). Effect of moisture absorption and temperature on quasi-static and fatigue behavior of nonwoven flax epoxy composite. *Composites Part B: Engineering, 166,* 31-40.
14. Moudood, A., Rahman, A., Khanlou, H. M., Hall, W., Öchsner, A. et al. (2019). Environmental effects on the durability and the mechanical performance of flax fiber/bio-epoxy composites. *Composites Part B: Engineering, 171,* 284-293.
15. Lu, M. M., Van Vuure, A. W. (2019). Improving moisture durability of flax fibre composites by using non-dry fibres. *Composites Part A: Applied Science and Manufacturing, 123,* 301-309.
16. Barjasteh, E., Nutt, S. R. (2012). Moisture absorption of unidirectional hybrid composites. *Composites Part A: Applied Science and Manufacturing, 43,* 158-164.
17. Scida, D., Assarar, M., Poilâne, C., Ayad, R. (2013). Influence of hygrothermal ageing on the damage mechanisms of flax-fibre reinforced epoxy composite. *Composites Part B: Engineering, 48,* 51-58.
18. Cherif, Z. E., Poilâne, C., Falher, T., Vivet, A., Ouail, N. et al. (2013). Influence of textile treatment on mechanical and sorption properties of flax/epoxy composites. *Polymer Composites, 34(10),* 1761-1773.
19. Saidane, E. H., Scida, D., Assarar, M., Ayad, R. (2016). Assessment of 3D moisture diffusion parameters on flax/epoxy composites. *Composites Part A: Applied Science and Manufacturing, 80,* 53-60.
20. Chilali, A., Assarar, M., Zouari, W., Kebir, H., Ayad, R. (2017). Effect of geometric dimensions and fibre orientation on 3D moisture diffusion in flax fibre reinforced thermoplastic and thermosetting composites, *Composites Part A: Applied Science and Manufacturing, 95,* 75-86.
21. Vaddadi, P., Nakamura, T., Singh, R. P. (2003). Transient hygrothermal stresses in fiber reinforced composites: a heterogeneous characterization approach. *Composites Part A: Applied Science and Manufacturing, 34 (8),* 719-730.
22. Vaddadi, P., Nakamura, T., Singh, R. P. (2003). Inverse analysis for transient moisture diffusion through fiber-reinforced composites. *Acta Materialia*, *51 (1),* 177-193.
23. Joliff, Y., Belec, L., Heman, M., Chailan, J. (2012). Experimental, analytical and numerical study of water diffusion in unidirectional composite materials-Interphase impact. *Computational Materials Science, 64,* 141-145.
24. Joliff, Y., Belec, L., Chailan, J. F. (2013). Modified water diffusion kinetics in an unidirectional glass/fibre composite due to the interphase area: Experimental, analytical and numerical approach. *Composite Structures, 97,* 296-303.
25. Peret, T., Clement, A., Freour, S., Jacquemin (2014). Numerical transient hygro-elastic analyses of reinforced Fickian and non-Fickian polymers. *Composite Structures, 116,* 395-403.
26. Peret, T., Clement, A., Freour, S., Jacquemin, F. (2017). Effect of mechanical states on water diffusion based on the free volume theory: numerical study of polymers and laminates used in marine application. *Composites Part B: Engineering, 118,* 54-66.
27. Regazzi, A., Léger, R., Corn, S., Ienny, P. (2016). Modeling of hydrothermal aging of short flax fiber reinforced composites. *Composites Part A: Applied Science and Manufacturing, 90,* 559-566.
28. Chilali, A., Zouari, W., Assarar, M., Kebir, H., Ayad, R. (2016). Analysis of the mechanical behaviour of flax

and glass fabrics-reinforced thermoplastic and thermoset resins. *Journal of Reinforced Plastics and Composites, 35,* 1217-1232.

29. Crank, J. (1986). *The mathematics of diffusion.* OUP Oxford.
30. Scida, D., Aboura, Z., Benzeggagh, M., Bocherens, E. (1998). Prediction of the elastic behaviour of hybrid and non-hybrid woven composites. *Composites Science and Technology, 57(12),* 1727-1740.
31. Halpin, J. C., Kardos, J. L. (1976). The Halpin-Tsai equations: a review. *Polymer Engineering & Science, 16 (5),* 344-352.
32. Woo, M., Piggott, M. (1988). Water absorption of resins and composites: IV.Water transport in fiber reinforced plastics. *Journal of Composites, Technology and Research, 10,* 20-24.
33. Bunsell, A. (1995). Hydrothermal aging of composite materials. *Revue de l'Institut Français du Pétrole, 50,* 61-67.
34. Kumosa, L., Benedikt, B., Armentrout, D., Kumosa, M. (2004). Moisture absorption properties of unidirectional glass/polymer composites used in composite (non-ceramic) insulators. *Composites Part A: Applied Science and Manufacturing, 35(9),* 1049-1063.
35. Arnold, J., Alston, S., Korkees, F. (2013). An assessment of methods to determine the directional moisture diffusion coefficients of composite materials. *Composites Part A: Applied Science and Manufacturing, 55,* 120-128.